ACS APPLIED MATERIALS & INTERFACES

Letter

www.acsami.org

Conducting, Self-Assembled, Nacre-Mimetic Polymer/Clay Nanocomposites

Roi Oskari Mäkiniemi,[†] Paramita Das,[†] Daniel Hönders,[†] Konrad Grygiel,[‡] Daniela Cordella,[§] Christophe Detrembleur,[§] Jiayin Yuan,[‡] and Andreas Walther*[,†]

[†]DWI-Leibniz-Institute for Interactive Materials, Forckenbeckstraße 50, 52056 Aachen, Germany

[‡]Max-Planck-Institute of Colloids and Interfaces, Am Mühlenberg 1, 14476 Potsdam, Germany

[§]Center for Education and Research on Macromolecules (CERM), Chemistry Department, University of Liege (ULg), Sart-Tilman, B6a, 4000 Liege, Belgium

Supporting Information

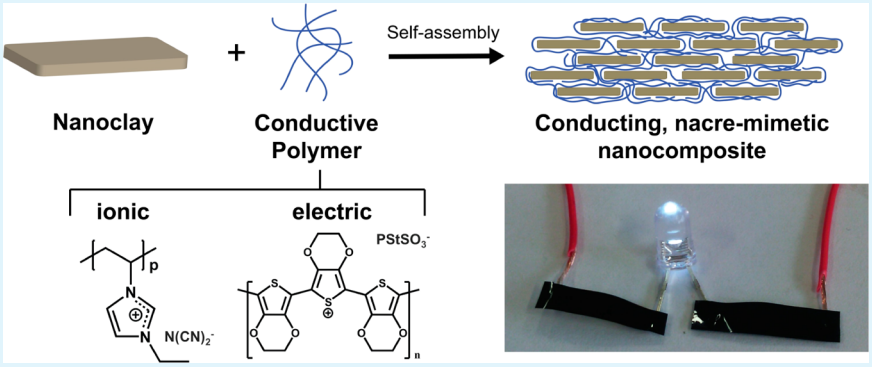

ABSTRACT: We demonstrate electrically and ionically conducting nacre-mimetic nanocomposites prepared using self-assembly of synthetic nanoclay in combination with PEDOT:PSS and a poly(ionic liquid) polymer from aqueous dispersions. The resulting nacre-mimetics show high degrees of mesoscale order and combine high stiffness and high strength. In terms of conductivities, the resulting hybrids exceed simple additive behavior and display synergetic conductivities due to high levels of interfaces and anisotropic conductivity pathways. The approach highlights the integration of relevant functionalities into stiff and strong bioinspired materials, and shows that synergetic properties beyond mechanical performance can be realized in advanced multifunctional nanocomposites using nacre-inspired design principles.

KEYWORDS: *nacre-mimetic nanocomposites, synergetic properties, PEDOT:PSS, poly(ionic liquid), nanoclay*

The hierarchical brick-and-mortar structure of nacre, in which 95 vol % aragonite platelets are held together by thin layers of biopolymer, has attracted great attention because of the exceptional mechanical properties and lightweight character.[1,2] Several strategies have emerged in the past decade to prepare nacre-inspired materials, most notably sequential deposition of hard and soft materials,[3,4] ice-templating and sintering of ceramic slurries followed by resin infusion,[5,6] or our self-assembly approach using concentration-induced self-ordering of polymer-coated nanoclay platelets.[7,8] In terms of nanoclay-based nacre-mimetics, most efforts have so far been focused on using natural montmorillonite (MTM) nanoclay in combination with classical water-soluble polymers, such as polyelectrolytes, poly(vinyl alcohol) or polysaccharides.[3,7,9,10] We recently reported in detail how to tailor the mechanical properties of self-assembled clay-based nacre-mimetics using synthetic nanoclays with different aspect ratios and polymers with tailored dynamics.[11−13] Although the use of water-soluble polymers requires special attention for high-humidity applications, the versatility of the waterborne process allows for the conceptual design of highly ordered materials with tailored properties and even new functionalities that are relevant for the engineering world.

The concept of conductive polymer composites based on electrically conductive inorganic fillers like carbon black,[14−16] graphite,[17] carbon nanotubes,[18,19] or graphene[20,21] is well-established, but intrinsically electrically, and ionically conductive polymers are hardly addressed in nanocomposite settings. Yet they are of special interest for their potential application as conductivity pathways in antistatic coatings, organic solar cells and LEDs, actuators and as solid electrolytes for batteries and fuel cells.[22,23] While the class of electrically conductive polymers has many well-studied examples with high electric conductivity, including polyanilines, polypyrroles and polythiophenes, such as poly(3,4-ethylenedioxythiophene)

Received: May 29, 2015
Accepted: July 15, 2015
Published: July 15, 2015

DOI: 10.1021/acsami.5b04676
ACS Appl. Mater. Interfaces 2015, 7, 15681−15685

Scheme 1. General Approach for the Waterborne Self-Assembly of Nacre-Mimetic Films Based on Sumecton (SUM) Nanoclay and Conducting Polymers[a]

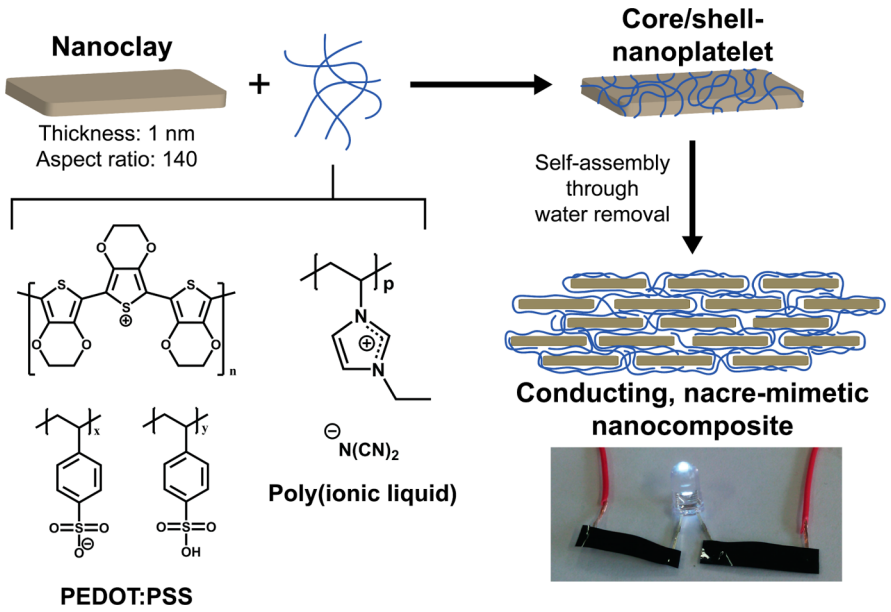

[a]PEDOT:PSS = Poly(3,4-ethylenedioxythiophene) polystyrenesulfonate; Poly(ionic liquid) = poly(1-ethyl-3-vinylimidazolium dicyanamide). The photograph at the bottom right shows a LED connected via conducting PEDOT:PSS/SUM nacre-mimetics and powered at 3.5 V.

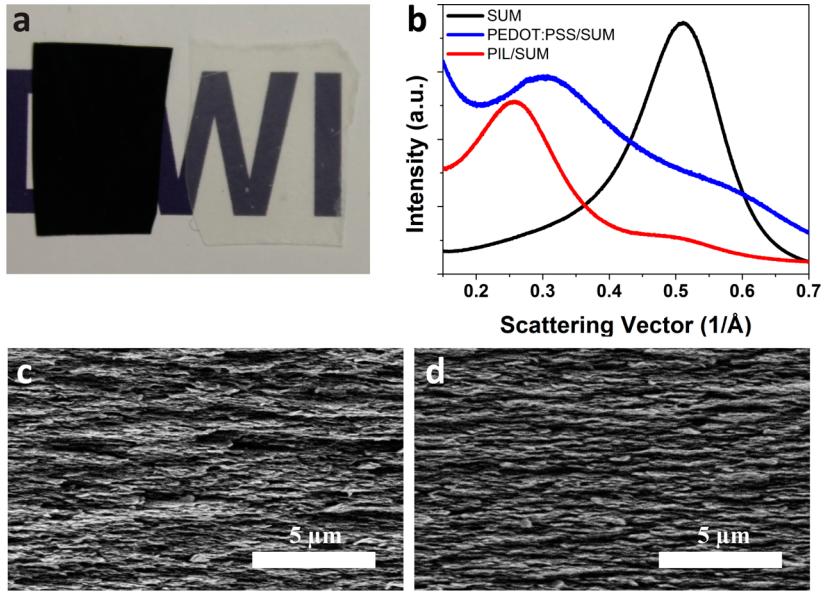

Figure 1. Structural characterization and macroscopic appearance. (a) Optical comparison of nacre-mimetic films based on PEDOT:PSS (black on left) and PILs (transparent on right). (b) Wide-angle X-ray diffractograms of the investigated systems. (c, d) SEM images of nacre-mimetic films based on (c) PEDOT:PSS and (d) PILs.

("PEDOT"), satisfactory ion conductivity can be found in a class of ionic polymers known as poly(ionic liquid)s (PILs). Structurally well-defined and tailored PILs allow to reach low glass transition temperatures, promoting a high chain mobility and thus increased ion conductivities.[24,25] However, the weak intermolecular interactions of PILs result in poor mechanical cohesion, limiting the applicability of these materials.

To combine the superior mechanical design principles of nacre-mimetics with the high electric or ion conductivity of the conductive polymers, we herein demonstrate a facile, aqueous self-assembly process of core/shell nanoplatelets, being either obtained by combination of nanoclay with PEDOT:PSS or with PILs.[7,8] As building blocks we chose PEDOT:PSS and poly(*N*-ethyl-3-vinylimidazolium dicyanamide) (the latter with number-average molecular weight, M_n = 14 kg/mol and 78 kg/mol; Scheme 1) for their high electric and ionic conductivities, respectively.[24,26] We selected a synthetic saponite nanoclay (Sumecton, "SUM") with an aspect ratio of 140 (determined by statistical image analysis using scanning electron microscopy; SEM) as the hard, reinforcing phase.[12] Such synthetic nanoclays have the advantage of (i) being free of colored contaminants, thus potentially allowing transparent nacre-mimetics, and (ii) freely delaminating into 1 nm thick sheets in aqueous dispersions. To coat a single layer of polymers onto

DOI: 10.1021/acsami.5b04676
ACS Appl. Mater. Interfaces 2015, 7, 15681−15685

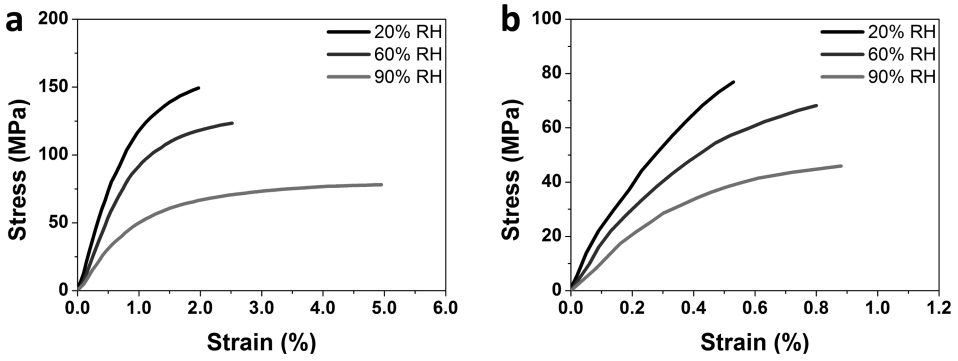

Figure 2. Tensile mechanical properties. Stress–strain curves for nacre-mimetic films based on (a) PEDOT:PSS/SUM and (b) PIL/SUM (M_n = 78 kg/mol) at different humidities (please see Table 1 for data on low M_n PIL/SUM).

the nanoclays, a ca. 0.4 wt % nanoclay dispersion is added slowly to a vigorously stirred 1.0 wt % polymer solution in water (final polymer/clay ratio = 67/33 w/w). This leads to polymer adsorption due to electrostatic complexation on the anionic basal planes (cationic PILs) and cationic rim regions (anionic PSS-coated PEDOT) of the nanoclay, as well as hydrophobic and van-der-Waals interactions interacting less specifically on the other parts of the nanoclay, respectively. To remove excess polymer, the mixtures are centrifuged, and redispersion of the sediment gives a dispersion of the core/shell-nanoplatelets.[8,12] Their hard/soft core/shell type character is decisive to deliver defined periodicities in the final nacre-mimetic materials. After film casting and drying overnight at 50 °C, macroscopically, mechanically coherent and flexible films of ca. 20 μm in thickness are obtained for both materials. For comparison, film casting of pure SUM gives extremely brittle films that can hardly be handled. The PIL/SUM nanocomposite film is nearly fully transparent (Figure 1a). This is a clear benefit of using the synthetic nanoclay over commonly used natural MTM nanoclay, which can only produce yellowish and translucent films. At the same time, the PEDOT:PSS/SUM film has an intense dark blue/black color, due to the integration of the conducting PEDOT:PSS, which has a dark bluish appearance in solution (Figure 1a). Elemental analysis gives 50 and 53 wt % of polymer within the final films for PEDOT:PSS/SUM and PIL/SUM, respectively. This is to some extent surprising as it confirms that both polymers, despite having opposite charges, integrate with similar amounts into the nanocomposite because of tight polymer adsorption on the nanoclay surfaces.

The self-ordering of the nanoclay platelets into layered structures can be confirmed by SEM and X-ray diffraction (Figure 1b–d). The SEM images show the desired layered and stratified orientation of the nanoclays, whereas XRD shows a well-defined restacking into exfoliated and ordered nanocomposites. The primary diffraction peak migrates from q^*_{SUM} = 0.51 Å^{-1} (d-spacing = 1.23 nm) for pure Sumecton nanoclay to $q^*_{PEDOT:PSS/SUM}$ = 0.30 Å^{-1} (d-spacing = 2.08 nm) and $q^*_{PIL/SUM}$ = 0.26 Å^{-1} (d-spacing = 2.45 nm), respectively. PEDOT:PSS/SUM shows a broader distribution of gallery spacings, which may be related to the partial nanoparticulate nature of the polymer suspension. In both cases, higher second order ($2q^*$) diffraction peaks occur, which for the PIL/SUM nanocomposite are closely in the range to the pristine nanoclay. In both cases, non-exfoliated nanoclay is nearly absent. This confirms a well-controlled structure formation given the rather high complexity of the functional polymers.

We investigated the mechanical properties using tensile tests in a chamber with controlled relative humidity (%RH, Figure 2, Table 1). The PEDOT:PSS/SUM nanocomposite exhibits a high Young's modulus (E) of 14.5 GPa and high tensile strength (σ_{UTS}) of ca. 150 MPa at 20%RH. A molecular weight dependency can be identified for the PIL/SUM nanocomposites. The PIL/SUM nacre-mimetic based on the lower molecular weight polymer (M_n = 14 kg/mol) shows an even higher stiffness of 17.2 GPa compared to the PEDOT:PSS/SUM, albeit with a lower tensile strength of ca. 56 MPa at the same humidity. However, by employing a PIL with a higher molecular weight (M_n = 78 kg/mol), both Young's modulus and tensile strength can be increased to 21.9 GPa and 77 MPa, respectively. By increasing the humidity inside the testing chamber, we can get a better view of the performance at relevant application conditions (e.g., 60%RH). Hydration of hydrophilic polymers screens the polymer/polymer interactions and increases the free volume of the polymer, thereby decreasing the glass transition temperature and thus the brittleness of the polymer.[10] This brittle-to-ductile transition of the mechanical properties can be observed for the PEDOT:PSS/SUM system as the Young's modulus and tensile strength decrease with increasing humidity, while the elongation more than doubles. Interestingly, the rather low internal cohesion of the PILs on the other hand only leads to a decrease in stiffness and prevents prolonged inelastic deformation when exposed to higher humidity.

Table 1. Averaged Mechanical Properties of the Investigated Systems

humidity (%RH)	stiffness E, (GPa)	strength, σ_{UTS} (MPa)	elongation, ε_b (%)
	PEDOT:PSS/SUM		
20	14.5 ± 1.9	148 ± 13	2.0 ± 0.8
60	10.5 ± 0.4	123 ± 7	2.4 ± 0.6
90	5.6 ± 0.3	75 ± 4	5.0 ± 1.1
	Low M_n PIL/SUM		
20	17.2 ± 2.0	56 ± 9	0.4 ± 0.2
60	12.9 ± 0.4	42 ± 8	0.5 ± 0.1
90	7.6 ± 0.4	34 ± 3	0.7 ± 0.1
	High M_n PIL/SUM		
20	21.9 ± 0.7	77 ± 15	0.6 ± 0.1
60	13.4 ± 0.4	67 ± 10	0.8 ± 0.1
90	6.3 ± 0.4	43 ± 2	0.9 ± 0.1

Next, we turn to the conductivity of the nanocomposites. In principal, nacre-mimetic design principles are appealing to

DOI: 10.1021/acsami.5b04676
ACS Appl. Mater. Interfaces 2015, 7, 15681–15685

make materials with anisotropic conductivity properties (in-plane vs out-of-plane) caused by the built-up of torturous pathways as a function of the aspect ratio and content of the aligned 2D nanoclays. However, the precise measurement of the out-of-plane electric conductivity for thin conducting films is associated with severe experimental problems because of the large influence of contact resistances, requiring sophisticated electrode setups.[27,28] Therefore, here we only report in-plane conductivities of the PEDOT:PSS/SUM films using a four-point-probe setup at 40%RH. The PEDOT:PSS used in this work exhibits an electric conductivity of ca. 440 S/m when cast into thin films, which can be increased to ca. 580 S/m when the film is tempered at 200 °C for 15 min because of sintering and coalescence of the PEDOT-rich nanograins.[29] The corresponding nacre-mimetics show a high conductivity of ca. 250 S/m before tempering, which corresponds roughly to the 50 wt % of PEDOT:PSS being integrated into the nanocomposites. Surprisingly, the conductivity increases drastically during tempering up to ca. 560 S/m. This is astonishing, as the value for pure PEDOT:PSS is almost fully recovered. This indicates that the nanoconfinement of the polymer may potentially lead to orientation of conducting domains or modulation of the PEDOT:PSS conduction band, which would be beneficial in generating highly conducting pathways during tempering. We used the electric conductivity in mechanically superior PEDOT:PSS/SUM nacre-mimetics to demonstrate the integration into a first functional device by connecting a power source via two ca. 2 cm long films to a small LED (wiring attached by conducting Ag paste; Scheme 1). The LED can be lit by switching on the power supply (photograph at ca. 3.5 V), thereby demonstrating efficient conduction.

The out-of-plane ionic conductivity of the PIL/SUM nacre-mimetic was investigated by electrochemical impedance spectroscopy at 25 °C and at 50%RH. To achieve a good contact between samples and electrodes, we deposited thin layers of Au/Pd on both sides of the specimen disks. Subsequently, the samples were conditioned for 24 h at the given environment before the impedance spectra were recorded. The calculated conductivity of a PIL/SUM blend at 1:1 polymer/clay weight ratio shows a value of 7.4 mS/m. Such results stay in agreement with data published in the literature, where enhanced ionic conductivity was observed for PIL/inorganic particle composites compared to the pure components. For example, grafting different amounts of PILs (ionic conductivity, σ = 1.8 mS/m) on the surface of silica nanoparticles (σ = 0.04 mS/m) resulted in composite materials with conductivity varying from 2.7 up to 10.4 mS/m, higher than individual PIL and silica.[30] This behavior can be related to increased ion mobility at the particle−polymer interface which, at a certain components ratio, leads to the formation of ionic channels reducing the resistance of the samples.[30,31]

In conclusion, we demonstrated the integration of attractive electric and ionic conductivity into mechanically robust self-assembled nacre-mimetics using highly functional polymers (PEDOT:PSS and PILs) in combination with a advanced synthetic nanoclay. The nanocomposites show attractive multifunctional property profiles with high transparency (in the case of PILs), high values of conductivity with synergetic increase of it, and with high stiffness and strength needed for structural materials and functional wear- and impact-resistant coatings, where the soft PIL is transformed into a stiff and strong nanocomposite. We believe that this generic approach will in the future give rise to materials with tailored anisotropic conductivities, new types of actuators and truly multifunctional bioinspired materials combining mechanical robustness with functionalities needed to advance functional materials. Moreover, the approach highlights that synergetic functional properties can be generated following nacre-mimetic design principles.

■ ASSOCIATED CONTENT

Supporting Information

Materials, methods, and experimental analysis. The Supporting Information is available free of charge on the ACS Publications website at DOI: 10.1021/acsami.5b04676.

■ AUTHOR INFORMATION

Corresponding Author

*E-mail: walther@dwi.rwth-aachen.de.

Notes

The authors declare no competing financial interest.

■ ACKNOWLEDGMENTS

We acknowledge financial support from the Volkswagen foundation. This work was performed in part at the Center for Chemical Polymer Technology, supported by the EU and North Rhine-Westphalia (EFRE 30 00 883 02). K.G. and D.C. thank the ITN Marie-Curie "Renaissance" funded by the People FP7 Program. A.W. thanks the BMBF for support in the Aquamat Research Group and gratefully acknowledges continuous support by M. Möller. C.D. is Research Director by F.R.S.-FNRS, Belgium.

■ ABBREVIATIONS

PEDOT:PSS, poly(3,4-ethylenedioxythiophene):polystyrene sulfonate
PIL, poly(ionic liquid)
SUM, sumecton

■ REFERENCES

(1) Jackson, A. P.; Vincent, J. F. V.; Turner, R. M. The Mechanical Design of Nacre. *Proc. R. Soc. London, Ser. B* **1988**, *234*, 415−440.
(2) Barthelat, F.; Espinosa, H. D. An Experimental Investigation of Deformation and Fracture of Nacre−Mother of Pearl. *Exp. Mech.* **2007**, *47*, 311−324.
(3) Tang, Z.; Kotov, N. A.; Magonov, S.; Ozturk, B. Nanostructured Artificial Nacre. *Nat. Mater.* **2003**, *3*, 413−418.
(4) Podsiadlo, P.; Kaushik, A. K.; Arruda, E. M.; Waas, A. M.; Shim, B. S.; Xu, J.; Nandivada, H.; Pumplin, B. G.; Lahann, J.; Ramamoorthy, A.; Kotov, N. A. Ultrastrong and Stiff Layered Polymer Nanocomposites. *Science* **2007**, *318*, 80−83.
(5) Deville, S.; Saiz, E.; Nalla, R. K.; Tomsia, A. P. Freezing as a Path to Build Complex Composites. *Science* **2006**, *311*, 515−518.
(6) Munch, E.; Launey, M. E.; Alsem, D. H.; Saiz, E.; Tomsia, A. P.; Ritchie, R. O. Tough, Bio-Inspired Hybrid Materials. *Science* **2008**, *322*, 1516−1520.
(7) Walther, A.; Bjurhager, I.; Malho, J.-M.; Pere, J.; Ruokolainen, J.; Berglund, L. A.; Ikkala, O. Large-Area, Lightweight and Thick Biomimetic Composites with Superior Material Properties via Fast, Economic, and Green Pathways. *Nano Lett.* **2010**, *10*, 2742−2748.
(8) Das, P.; Schipmann, S.; Malho, J.-M.; Zhu, B.; Klemradt, U.; Walther, A. Facile Access to Large-Scale, Self-Assembled, Nacre-Inspired, High-Performance Materials with Tunable Nanoscale Periodicities. *ACS Appl. Mater. Interfaces* **2013**, *5*, 3738−3747.
(9) Yao, H.-B.; Tan, Z.-H.; Fang, H.-Y.; Yu, S.-H. Artificial Nacre-like Bionanocomposite Films from the Self-Assembly of Chitosan−Montmorillonite Hybrid Building Blocks. *Angew. Chem., Int. Ed.* **2010**, *49*, 10127−10131.

DOI: 10.1021/acsami.5b04676
ACS Appl. Mater. Interfaces 2015, 7, 15681−15685

(10) Verho, T.; Karesoja, M.; Das, P.; Martikainen, L.; Lund, R.; Alegría, A.; Walther, A.; Ikkala, O. Hydration and Dynamic State of Nanoconfined Polymer Layers Govern Toughness in Nacre-mimetic Nanocomposites. *Adv. Mater.* **2013**, *25*, 5055−5059.
(11) Shao, Y.; Zhao, H.-P.; Feng, X.-Q.; Gao, H. Discontinuous Crack-Bridging Model for Fracture Toughness Analysis of Nacre. *J. Mech. Phys. Solids* **2012**, *60*, 1400−1419.
(12) Das, P.; Malho, J.-M.; Rahimi, K.; Schacher, F. H.; Wang, B.; Demco, D. E.; Walther, A. Nacre-Mimetics with Synthetic Sanoclays up to Ultrahigh Aspect Ratios. *Nat. Commun.* **2015**, *6*, 5967.
(13) Zhu, B.; Jasinski, N.; Benitez, A.; Noack, M.; Park, D.; Goldmann, A. S.; Barner-Kowollik, C.; Walther, A. Hierarchical Nacre-Mimetics with Synergistic Mechanical Properties by Control of Molecular Interactions in Self-Healing Polymers. *Angew. Chem., Int. Ed.* **2015**, *54*, 8653−8657.
(14) Medalia, A. I. Electrical Conduction in Carbon Black Composites. *Rubber Chem. Technol.* **1986**, *59*, 432−454.
(15) Sumita, M.; Sakata, K.; Asai, S.; Miyasaka, K.; Nakagawa, H. Dispersion of Fillers and the Electrical Conductivity of Polymer Blends Filled with Carbon Black. *Polym. Bull.* **1991**, *25*, 265−271.
(16) Connor, M. T.; Roy, S.; Ezquerra, T. A.; Baltá Calleja, F. J. Broadband ac Conductivity of Conductor-Polymer Composites. *Phys. Rev. B: Condens. Matter Mater. Phys.* **1998**, *57*, 2286−2294.
(17) Zheng, W.; Wong, S.-C. Electrical Conductivity and Dielectric Properties of PMMA/expanded Graphite Composites. *Compos. Sci. Technol.* **2003**, *63*, 225−235.
(18) Wu, M.; Shaw, L. L. On the Improved Properties of Injection-Molded, Carbon Nanotube-Filled PET/PVDF Blends. *J. Power Sources* **2004**, *136*, 37−44.
(19) Regev, O.; ElKati, P. N. B.; Loos, J.; Koning, C. E. Preparation of Conducting Nanotube-Polymer Composites Using Latex Technology. *Adv. Mater.* **2004**, *16*, 248−251.
(20) Stankovich, S.; Dikin, D. A.; Dommett, G. H. B.; Kohlhaas, K. M.; Zimney, E. J.; Stach, E. A.; Piner, R. D.; Nguyen, S. T.; Ruoff, R. S. Graphene-Based Composite Materials. *Nature* **2006**, *442*, 282−286.
(21) Kuilla, T.; Bhadra, S.; Yao, D.; Kim, N. H.; Bose, S.; Lee, J. H. Recent Advances in Graphene Based Polymer Composites. *Prog. Polym. Sci.* **2010**, *35*, 1350−1375.
(22) Groenendaal, L.; Jonas, F.; Freitag, D.; Pielartzik, H.; Reynolds, J. R. Poly(3,4-ethylenedioxythiophene) and Its Derivatives: Past, Present, and Future. *Adv. Mater.* **2000**, *12*, 481−494.
(23) Yuan, J.; Antonietti, M. Poly(ionic liquid)s: Polymers Expanding Classical Property Profiles. *Polymer* **2011**, *52*, 1469−1482.
(24) Green, M. D.; Salas-de la Cruz, D.; Ye, Y.; Layman, J. M.; Elabd, Y. A.; Winey, K. I.; Long, T. E. Alkyl-Substituted N-Vinylimidazolium Polymerized Ionic Liquids: Thermal Properties and Ionic Conductivities. *Macromol. Chem. Phys.* **2011**, *212*, 2522−2528.
(25) Shaplov, A. S.; Marcilla, R.; Mecerreyes, D. Recent Advances in Innovative Electrolytes based on Poly(ionic liquid)s. *Electrochim. Acta* **2015**, DOI: 10.1016/j.electacta.2015.03.038.
(26) Jonas, F.; Krafft, W.; Muys, B. Poly(3, 4-ethylenedioxythiophene): Conductive Coatings, Technical Applications and Properties. *Macromol. Symp.* **1995**, *100*, 169−173.
(27) Gijs, M. A. M.; Giesbers, J. B.; Lenczowski, S. K. J.; Janssen, H. H. J. M. New Contacting Technique for Thin Film Resistance Measurements Perpendicular to the Film Plane. *Appl. Phys. Lett.* **1993**, *63*, 111−113.
(28) Wei, Q.; Mukaida, M.; Kirihara, K.; Ishida, T. Experimental Studies on the Anisotropic Thermoelectric Properties of Conducting Polymer Films. *ACS Macro Lett.* **2014**, *3*, 948−952.
(29) Huang, J.; Miller, P. F.; de Mello, J. C.; de Mello, A. J.; Bradley, D. D. C. Influence of Thermal Treatment on the Conductivity and Morphology of PEDOT/PSS Films. *Synth. Met.* **2003**, *139*, 569−572.
(30) Wang, P.; Zhou, Y.-N.; Luo, J.-S.; Luo, Z.-H. Poly(ionic liquid)s-based Nanocomposite Polyelectrolytes with Tunable Ionic Conductivity Prepared via SI-ATRP. *Polym. Chem.* **2014**, *5*, 882−891.
(31) Willa, C.; Yuan, J.; Niederberger, M.; Koziej, D. When Nanoparticles Meet Poly(Ionic Liquid)s: Chemoresistive CO_2 Sensing at Room Temperature. *Adv. Funct. Mater.* **2015**, *25*, 2537−2542.

DOI: 10.1021/acsami.5b04676
ACS Appl. Mater. Interfaces 2015, 7, 15681−15685